Competitive coexistence in stoichiometric chaos

Bo Deng[a] and Irakli Loladze[b]
Department of Mathematics, University of Nebraska-Lincoln, Lincoln, Nebraska 68588, USA

(Received 24 January 2007; accepted 3 June 2007; published online 21 August 2007)

Classical predator-prey models, such as Lotka-Volterra, track the abundance of prey, but ignore its quality. Yet, in the past decade, some new and occasionally counterintuitive effects of prey quality on food web dynamics emerged from both experiments and mathematical modeling. The underpinning of this work is the theory of ecological stoichiometry that is centered on the fact that each organism is a mixture of multiple chemical elements such as carbon (C), nitrogen (N), and phosphorus (P). The ratios of these elements can vary within and among species, providing simple ways to represent prey quality as its C:N or C:P ratios. When these ratios modeled to vary, as they frequently do in nature, seemingly paradoxical results can arise such as the extinction of a predator that has an abundant and accessible prey. Here, for the first time, we show analytically that the reduction in prey quality can give rise to chaotic oscillations. In particular, when competing predators differ in their sensitivity to prey quality then all species can coexist via chaotic fluctuations. The chaos generating mechanism is based on the existence of a junction-fold point on the nullcline surfaces of the species. Conditions on parameters are found for such a point, and the singular perturbation method and the kneading sequence analysis are used to demonstrate the existence of a period-doubling cascade to chaos as a result of the point. © *2007 American Institute of Physics*. [DOI: 10.1063/1.2752491]

Predator-prey or consumer-resource dynamics is central to ecological complexity. Critical to all biomasses lies the mass balance law governing abiotic elements flowing through the species of ecological systems. Not only are the component fluxes in quantity important to the species but also the relative ratios of the elements of which individual species may have their own preferred composition. The question is: To what extent does the elemental composition of a resource influence its consumer's population? Adding to our understanding about ecological complexity we will demonstrate here that a simple food web can be driven to chaotic oscillation in population by just one consumer's sensitivity to the composition of only two elements of its resource.

I. INTRODUCTION

"Eating more prey never hurts predator growth" is one of the old adages in population dynamics. It goes back to Lotka-Volterra predator-prey models. This assumption is of twofold: predation and growth. The Lotka-Volterra models assumed that predator captures prey linearly (this response is known as Holling type I). Different predator responses were introduced later to account for more realistic situations, such as the cases where the capture rates can be saturated (Holling types II, III, IV). However, in all nonstoichiometric cases consuming more prey always translates into positive growth rates for predators. Interestingly, Lotka[1] himself hinted that this need not be true. As a physical chemist he realized that a prey and a predator do not "operate with a single working substance, but with a complex variety of such substances, a fact which has certain important consequences." Examples of such consequences were found in the past decade, when the theory of biological stoichiometry was applied to predator-prey interactions. Biological stoichiometry embraces and extends Lotka's idea of "multiple working substances"—it considers species not just as biomasses but as assemblages of multiple essential elements. The fact that the proportions of essential elements can vary within and between species can have some profound effects on species interactions.

For example, both experiments[2–4] and theoretical models[5–8] showed that when the quality of phytoplankton drops (often expressed as phosphorus to carbon, P:C, ratio), the growth of its predator, zooplankton, declines even as it consumes more algae. The reason is that the low quality of prey, as measured by its P content, hampers the growth of zooplankton that has a higher P:C ratio than its food. This effect can lead to unusual dynamical outcomes, which include deterministic extinction of the predator at a very high prey density (and a very low prey quality), stabilization of predator-prey oscillations, and coexistence of two predators on one prey at a steady state.[9] Stoichiometric models reflect the fact that prey is an assemblage of multiple elements required by its consumers albeit in different ratios. The same prey can be of good quality to one consumer and of bad quality to another. This interplay between quantity and quality should expand possibilities of coexistence beyond stable equilibriums.

Here, for the first time to our knowledge, we prove that stoichiometry can lead to coexistence via chaotic fluctuations. The idea that fluctuations can enhance coexistence is

[a]Electronic mail: bdeng@math.unl.edu
[b]Electronic mail: iloladze@math.unl.edu

 © 2007 American Institute of Physics

Downloaded 10 Sep 2007 to 129.93.181.195. Redistribution subject to AIP license or copyright, see http://chaos.aip.org/chaos/copyright.jsp

not new. Armstrong and McGehee[10,11] showed that n consumers can coexist on fewer than n resources via periodic fluctuations. Huisman and Weissing[12] numerically showed that the competition of phytoplankton species for three or more abiotic resources can give rise to chaos, where many species coexist on a handful of abiotic resources. We show here both analytically and numerically that chaos can arise when two consumers compete for just one biotic resource and it happens when the resource is of bad quality to at least one of the consumers.

II. MODEL

For a detailed derivation and justification of the model, we refer readers to Ref. 9. Here we briefly describe the model of two consumers exploiting one prey in a system with no spatial heterogeneity or external variability. We do not assume, *a priori*, that higher prey density should always benefit consumer growth; instead, mass balance laws will determine consumer growth in our model. To have some concrete system in mind, we can think of the prey as a single species of alga, while the consumers are two distinct zooplankton species, all placed in a well-mixed system open only to light and air.

For simplicity, we will model only two chemical elements, P and C. The choice of C is clear, because this element comprises the bulk of the dry weight of most organisms. Instead of P, however, one can choose any other element as long as it is essential to all species in the system (e.g., N, S, or Ca). Our model will reflect the following stoichiometric assumptions:

(1) The prey's P:C ratio varies, but never falls below a minimum q (mg P/mg C).
(2) The two consumers maintain a constant P:C ratio, s_1 and s_2 (mg P/mg C), respectively.
(3) The system is closed for P, with a total of P concentration in mg P/L, which is divided into two pools: P in the consumers and the rest as potentially available for the prey.

From these assumptions it follows that P available for the prey at any given time is

$$(P - s_1Y_1 - s_2Y_2)$$

in mg P/L, where Y_1, Y_2 denote the consumer densities in milligrams of C per liter, i.e., mg C/L. Recalling that P:C in the prey should be at least q (mg P/mg C), one obtains that the prey density cannot exceed $(P-s_1Y_1-s_2Y_2)/q$ (mg C/L).

In addition, prey growth will be limited by light. Let K represent light limitation in the following way: Suppose that we fix light intensity at a certain value, then let the prey (which is a photoautotroph) grow with no consumers but with ample nutrients. The resource density will increase until self-shading ultimately stabilizes it at some value, K. Thus, every K value corresponds to a specific limiting light intensity and we can model the influence of higher light intensity as having the effect of raising K, all else being equal.[6] Following Liebig's law of the minimum, the combination of light and P limits the carrying capacity of the prey to

$$\min\left(K, \frac{P - s_1Y_1 - s_2Y_2}{q}\right).$$

To determine the prey's P:C at any given time, we follow Andersen[1] by assuming that the prey can absorb all potentially available P, which means that the prey's P:C (mg P:mg C) at any time is

$$(P - s_1Y_1 - s_2Y_2)/X, \tag{1}$$

where X denotes the prey density in mg C/L.

Note that we do not impose the maximal P quota on the prey, thus its P:C can become potentially unbounded for small X according to (1). As we will show later, this property does not have undesirable effects on the dynamics, because when the prey's P:C exceeds that of the consumers' (i.e., $>\max\{s_1, s_2\}$), the consumers become limited by C and the prey's P:C, however large it is, becomes dynamically irrelevant.

While prey stoichiometry varies according to (1), each consumer maintains its constant (homeostatic) P:C, s_i. If the prey's P:C ratio is $>s_i$, then the ith consumer converts consumed prey with the maximal (in C terms) efficiency, which we denote as e_i, and egests or excretes any excess of ingested P. If the prey's P:C is $<s_i$, then the ith consumer wastes the excess of ingested C. This waste is assumed to be proportional to the ratio of prey's P:C to ith consumer's P:C (Ref. 1), which reduces the growth efficiency in C terms. The following minimum function provides the simplest way, based strictly on mass balance laws, to capture such effects of variable prey quality on consumer growth efficiency:

$$e_i \min\left(1, \frac{(P - s_1Y_1 - s_2Y_2)/X}{s_i}\right). \tag{2}$$

Thus, e_1 and e_2 are the maximal growth efficiencies (conversion rates or yield constants) of converting ingested prey biomass into consumer biomasses. They are achieved only when prey quality is good relative to consumer needs. The mass balance law requires that $e_1<1$ and $e_2<1$. (An alternative formulation that does not use minimum functions is possible using the concept of synthesizing units.[7])

Incorporating these assumptions above and others to be specified below, we consider in this paper the following model:

$$\begin{aligned}
\frac{dX}{dt} &= rX\left(1 - \frac{X}{\min\{K, (P - s_1Y_1 - s_2Y_2)/q\}}\right) - \frac{c_1X}{a_1 + X}Y_1 \\
&\quad - \frac{c_2X}{a_2 + X}Y_2, \\
\frac{dY_1}{dt} &= e_1 \min\left\{1, \frac{(P - s_1Y_1 - s_2Y_2)/X}{s_1}\right\}\frac{c_1X}{a_1 + X}Y_1 - d_1Y_1, \\
\frac{dY_2}{dt} &= e_2 \min\left\{1, \frac{(P - s_1Y_1 - s_2Y_2)/X}{s_2}\right\}\frac{c_2X}{a_2 + X}Y_2 - d_2Y_2,
\end{aligned} \tag{3}$$

where again X, Y_1, and Y_2 are the densities of the prey and the two consumers, respectively (in mg C/L). Also, param-

Downloaded 10 Sep 2007 to 129.93.181.195. Redistribution subject to AIP license or copyright, see http://chaos.aip.org/chaos/copyright.jsp

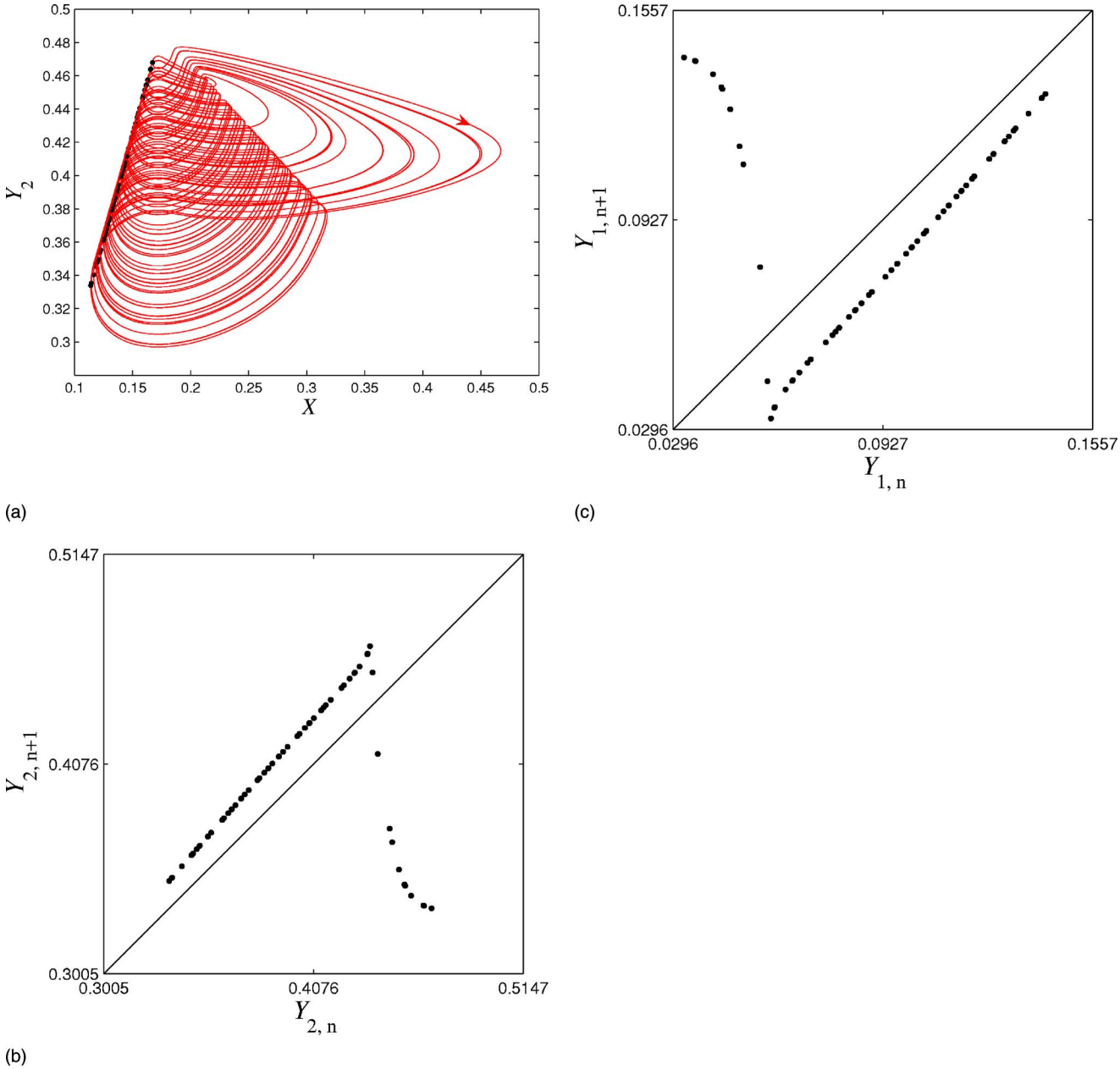

FIG. 1. (Color online) (a) A chaotic attractor of Eq. (3) projected to the XY_2 plane with parameter values: $r=1.4$, $K=0.64$, $c_1=0.81$, $c_2=0.75$, $a_1=0.25$, $a_2=0.28$, $e_1=0.7$, $e_2=0.85$, $P=0.026$, $q=0.0038$, $s_1=0.025$, $s_2=0.037$, $d_1=0.2$, $d_2=0.18$. (b) The return map in variable Y_2. (c) The same return map in variable Y_1. All variables shown are scaled according to (5).

eter r is the intrinsic growth rate of the prey (day^{-1}). Parameters d_1 and d_2 are the specific loss rates of the consumers that include respiration and death (day^{-1}). Holling type II functional response is assumed for consumer ingestion rates, with c_i being the saturation ingestion rates and a_i being the half-saturation densities.

Figure 1 gives a numerical diagnosis of the chaos attractor. The attractor shown in Fig. 1(a) has two distinct features: spirals around a horn and the returning of the spirals from the tip of the horn to the opening of the horn. Without the returning of the spirals the attractor would settle down to a periodic oscillation qualitatively similarly to a classical, two-dimensional (2D) predator-prey oscillation: more predators follow more prey. The stoichiometric effect of the dynamics lies precisely in this returning feature of the attractor: fewer predators follow more prey. That is, in the tip-to-opening journey, the system has an excessive carbon in X for consumer Y_2 and the excess negatively impacts on Y_2's population density. Figures 1(b) and 1(c) are return maps of the attractors in variable Y_2, Y_1, respectively. They are defined whenever the orbit hits a local minimum in X, showing as dots in Fig. 1(a). Notice that the return maps are approximately one-dimensional (1D) and have a unique critical point. The critical point separates each consumer variable range into two phases. In the case of Y_2 from Fig. 1(b), the subinterval left of the maximum point corresponds to the classical predator-prey oscillation, whereas the subinterval right of the maximum point corresponds to the stoichiometric effect of the system. The stoichiometric phase for Y_1 from Fig. 1(c) is the subinterval left of the minimum point in

Downloaded 10 Sep 2007 to 129.93.181.195. Redistribution subject to AIP license or copyright, see http://chaos.aip.org/chaos/copyright.jsp

which the surge in Y_1's density is the direct result of a greater resource in X made available by Y_2's decline; one competitor's loss is another competitor's gain.

The return map plots also suggest a near two-dimensional flow structure of the attractor. The analytical objective of this paper is to understand the stoichiometric effect that leads to such low-dimensional chaotic attractors in the model. The main theoretical result of this paper can be stated roughly as follows:

Theorem 1. *There is a parameter region through which a one-parameter bifurcation, primarily in varying parameter* $\delta_1=d_1/(e_1c_1)$*, gives rise to a period-doubling cascade scenario of chaos generation, and the corresponding dynamics must go through a phase in which increasing X decreases* Y_2.

A precise restatement of this theorem is given later in theorem 2.

III. ANALYSIS

We will use the method of multi-time-scale analysis, which is technically known as the singular perturbation method in the field of dynamical systems. The method is geometrical in nature. It facilitates a geometric construction of the chaotic attractor. As a result, we will have to specify the corresponding parameter region for the attractor. An outline of the analysis is as follows. In Sec. III A a further simplification of the model, as well as its nondimensionalization, are carried out. To keep track of the many geometric objects throughout the paper, a useful notational taxonomy is introduced in Sec. III B. The special cases of two-dimensional subsystems in X,Y_1 and X,Y_2, respectively, are summarized from the literature in Sec. III C to gradually introduce some of the terminology and more importantly a rudimentary treatment of the singular perturbation method. Various conditions are specified along the way to zoom in on the parameter region wanted. In Sec. III D the full three-dimensional (3D) system is pieced together from lower-dimensional subsystems in XY_1 and XY_2, respectively. Last, a one-dimensional return map is constructed in Sec. III E and its dynamics is shown to be chaotic. A precise statement of the main result as well as a proof are also given there.

A. Model simplification

Although the stoichiometric inclusion of phosphorus in the model is absolutely essential for its chaotic dynamics, not all phosphorus related effects are equally important. One task is to find out the minimum ingredients for the underlining dynamics. It turns out that it only suffices to consider the case in which only one consumer is truly affected by the stoichiometric consideration. As a result, in the effective region of the stoichiometric chaos under consideration, the model Eq. (3) has a constant carrying capacity for the resource and a constant efficiency factor for one of the consumers, which we will take to be Y_1. Because of this, we will remove these nonlinearities from the equations for simplicity and only consider the following equivalent equations from now on:

$$\frac{dX}{dt}=rX\left(1-\frac{X}{K}\right)-\frac{c_1X}{a_1+X}Y_1-\frac{c_2X}{a_2+X}Y_2$$

$$\frac{dY_1}{dt}=e_1\frac{c_1X}{a_1+X}Y_1-d_1Y_1 \tag{4}$$

$$\frac{dY_2}{dt}=e_2\min\left\{1,\frac{(P-s_1Y_1-s_2Y_2)/X}{s_2}\right\}\frac{c_2X}{a_2+X}Y_2-d_2Y_2.$$

As a necessary first step for mathematical analysis, we nondimensionalize Eq. (4) so that the new dimensionless system contains a minimum number of parameters. Following the same scaling idea of Ref. 13, the following changes of variables and parameters are used for the nondimensionalization:

$$t\to e_2c_2t,\quad x=\frac{X}{K},\quad y_1=\frac{Y_1}{rK/c_1},\quad y_2=\frac{Y_2}{rK/c_2}, \tag{5}$$

$$\beta_i=\frac{a_i}{K},\quad \delta_i=\frac{d_i}{e_ic_i}\quad \sigma_i=\frac{s_irK}{c_iP},\quad \kappa=\frac{Ks_2}{P},\quad \epsilon=\frac{e_2c_2}{r},$$

$$\zeta=\frac{e_1c_1}{e_2c_2}.$$

In the new variables and parameters the equations are transformed into the following dimensionless form:

$$\epsilon\frac{dx}{dt}=x\left(1-x-\frac{y_1}{\beta_1+x}-\frac{y_2}{\beta_2+x}\right),$$

$$\frac{dy_1}{dt}=\zeta y_1\left(\frac{x}{\beta_1+x}-\delta_1\right),$$

$$\frac{dy_2}{dt}=y_2\left(\min\left\{1,\frac{(1-\sigma_1y_1-\sigma_2y_2)}{\kappa x}\right\}\frac{x}{\beta_2+x}-\delta_2\right).$$

The rationale for this particular choice of nondimensionalization is as follows. The dimensionless prey variable, $x=X/K$, measures the fraction of the prey density against its best possible total K. The scaling of consumer $y_1=Y_1/M_1$ with $M_1=rK/c_1$ is motivated by this relation: $rK=c_1M_1$. Because r is the maximum per capita growth rate of the prey, and c_1 is the maximum per capita capture rate by the predator Y_1, then M_1 can be interpreted as the predation capacity in the sense that the best possible catch c_1M_1 by M_1 amount of the predator equalizes the best possible amount in prey regeneration rK. Thus y_1 is the fraction of Y_1's density against its predation capacity M_1. The same explanation applies to the dimensionless density y_2.

Parameters β_1,β_2 are the dimensionless semisaturation constants, which are the fractions of the dimensional semisaturation constants of the predators against prey's carrying capacity K. Parameters δ_1,δ_2 are the dimensionless or relative death rates; each is the fraction of the corresponding predator's minimum per capita death d_i rate to its maximum per capita birth rate e_ic_i. As a necessary condition for species

Downloaded 10 Sep 2007 to 129.93.181.195. Redistribution subject to AIP license or copyright, see http://chaos.aip.org/chaos/copyright.jsp

survival, the former must be smaller than the latter. Thus we will make it as a default assumption that $0<\delta_i<1$ for nontriviality.

Parameter σ_1 is the dimensionless P:C ratio for predator Y_1. The interpretation follows by noticing that $\sigma_1=s_1/[c_1P/(rK)]$ and that the ratio $c_1P/(rK)$ is the P:C ratio of predator Y_1's maximum per capita consumption rate of phosphorus c_1P against prey's maximum per capita regeneration rate of carbon. The same explanation applies to σ_2. Parameter $\kappa=K/(P/s_2)$ is the dimensionless fraction of prey's carrying capacity in carbon against predator Y_2's carrying capacity in carbon.

Parameter $\epsilon=e_2c_2/r$ is the Y_2X prolificacy, measuring the maximum growth rate of Y_2 against that of X. Similarly, parameter $\zeta=e_1c_1/(e_2c_2)$ is the Y_1Y_2-prolificacy parameter. By the theory of allometry,[14,15] these ratios correlate reciprocally well with the fourth roots of the ratios of X's body mass to Y_2's body mass and, respectively, Y_2's body mass to Y_1's body mass. Thus, ϵ is usually of a small order such as in the case of phytoplankton-zooplankton relation under consideration. By the same reasoning parameter ζ may or may not be small because Y_1, Y_2 are in the same trophic level. We also point out that $1(=e_2c_2t)$ unit in the new dimensionless time scale equals $t=1/(e_2c_2)$ units in the original time scale, which represents the average time interval between birth of Y_2.

The number of parameters is reduced from 13 to 9 dimensionless parameters. This means every point from the nine-dimensional dimensionless parameter space corresponds to a four-dimensional subspace in the original 13-dimensional system parameter space for which the dynamics of the system are identical when the density variables and time are scaled properly. This is a key point of nondimensionalization and equivalent dynamics.

To minimize the usage of subscripts, we will use from now on

$$y=y_1, \quad z=y_2,$$

and the equations are

$$\epsilon\frac{dx}{dt}=x\left(1-x-\frac{y}{\beta_1+x}-\frac{z}{\beta_2+x}\right):=xf(x,y,z),$$

$$\frac{dy}{dt}=\zeta y\left(\frac{x}{\beta_1+x}-\delta_1\right):=\zeta yg(x,y,z), \tag{6}$$

$$\frac{dz}{dt}=z\left(\min\left\{1,\frac{(1-\sigma_1y-\sigma_2z)}{\kappa x}\right\}\frac{x}{\beta_2+x}-\delta_2\right):=zh(x,y,z).$$

Chaotic coexistence has not been observed in the same system without the second element (phosphorus in our case). The goal is to understand how stoichiometry leads to competitive coexisting chaos. It turns out that such chaotic structure can persist in the limit $\epsilon\to0$ for which the limiting attractor is referred to as the singular attractor. The importance of studying singular attractors has long been recognized in the studies of dynamics systems because they can be considered as the origins of the underlying dynamics, retaining most essential information. The remaining sections are devoted to the description and analysis of the singular chaotic attractor, emphasizing the mechanistic role of stoichiometry.

To a greater extent, the study of an ecological system is to understand its species' temporal population dynamics. Being able to unlock the underlining mechanisms for population boom and bust is a requisite of any effective method. For continuous models such as the one under consideration, such a method inevitably has to deal with the nullclines of the models simply because it is through the nullclines that populations switch between being increasing and decreasing. The singular perturbation method that we will use indeed centers its analysis around the nullclines. It is both geometrical and global in nature, and has been proved extremely effective in understanding chaotic attractors (see Refs. 13 and 16–20).

B. Notation convention

A few notational rules are used for this paper, following a similar convention adopted in Ref. 13. Letter p is always used for point(s). Depending on the context, it can be a single point, or a *set* of points, which form a curve or a surface. It is usually identified by a subscript in a string of letters. The first one or two subscript letters have to be the variables x,y,z, indicating the nullcline(s) which the point belongs to or is associated with. The remaining subscript string is usually an acronym characterizing the point. For example, p_{xdc} can be read as a "point from the *d*escending *c*arrying-capacity" (to be explained later) "of the x nullcline." When the subscript has a two-letter variable prefix, the order is usually important. For example, p_{xzgt} means the intersection of the x nullcline with the plane p_{zgt}—the *g*rowing *t*hreshold of the z nullcline. Although the operation of intersection is order independent, the analysis that uses the point is order dependent. It means the consideration of the x nullcline precedes the consideration of the z nullcline, and it is the restriction of the system on the x nullcline first that the z nullcline of the restricted system is considered. Transposing the prefix shifts the emphasis and the order of analysis completely. One minor exception to these general rules is the notation p_{xyz} for the equilibrium point of the system that is the intersection of all nontrivial nullclines.

C. Multi-time-scale analysis: 2D cases

The dimensionless equations (6) can have three time scales if both ϵ and ζ are small: $0<\epsilon\ll1, 0<\zeta\ll1$, in which case the time scale is fast for x, intermediate for z, and slow for y. Because of the allometry theory, we will always assume that x is the fastest regardless of the relative scale between y and z. In addition, it turns out that the chaotic singular attractor will exist at the ordered singular limit $\epsilon\to0$ followed by $\zeta\to0$. We formalize these two considerations in the following.

Condition 1. *The trophic time diversification and the asymmetry competition prolificacy condition:* $e_1c_1\ll e_2c_2\ll r$, *equivalently,* $0<\epsilon\ll1$, $0<\zeta\ll1$.

We will begin our analysis by first considering the 2D subsystems with $z=0$ and $y=0$ separately, and then use them

Downloaded 10 Sep 2007 to 129.93.181.195. Redistribution subject to AIP license or copyright, see http://chaos.aip.org/chaos/copyright.jsp

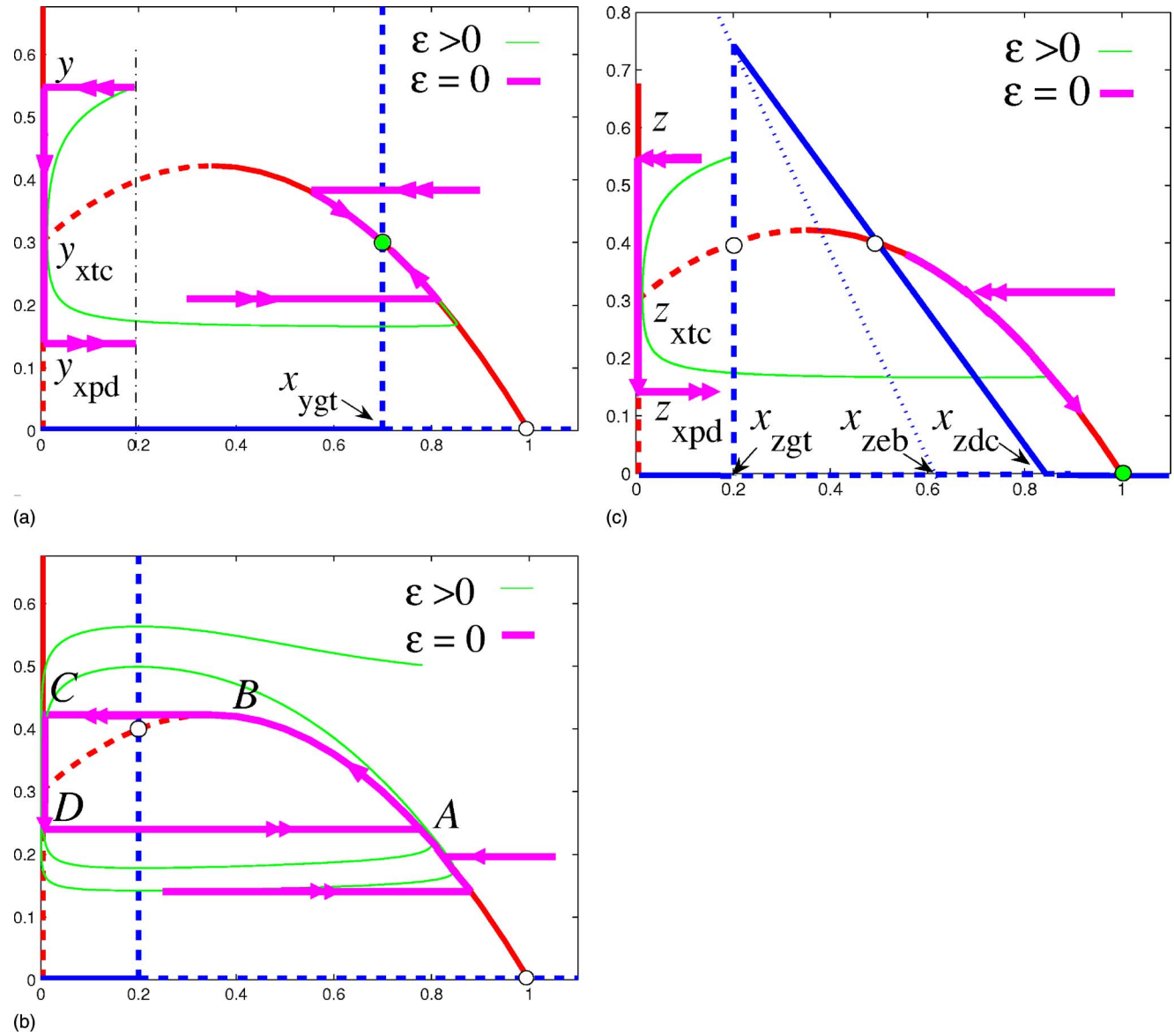

FIG. 2. (Color online) (a) Typical singular orbits in the case of stable xy-equilibrium state for which $x_{xcf}<x_{ygt}<1$. See text for the derivation of y_{xpd} on the phenomenon of Pontryagin's delay of loss of stability at which a boom in x population occurs although the recovery starts immediately after its crossing the transcritical point y_{xtc}. (b) A typical xy singular limit cycle and its relaxed cycle for $0<\epsilon\ll 1$ in the case $0<x_{ygt}<x_{xcf}$. (c) The xz subsystem in the case of $x_{zgt}<x_{zeb}<x_{zdc}<1$. The dynamical consequence is that without the competition from y, z eventually dies off from a detrimentally low P:C ratio when exposed to the resource capacity on p_{xdc}.

as building blocks to piece together the 3D dynamics. Working with the simpler subsystems should allow us to fix the needed notation and concept quicker.

1. Singular dynamics without stoichiometric limitation

To begin, Fig. 2 illustrates some essential elements of the singularly perturbed subsystems with $z=0$ and $y=0$. The xy system in the absence of z is a singular perturbed system,

$$\epsilon\frac{dx}{dt}=x\left(1-x-\frac{y}{\beta_1+x}\right)=xf(x,y,0),$$

$$\frac{dy}{dt}=\zeta y\left(\frac{x}{\beta_1+x}-\delta_1\right)=\zeta yg(x,y,0),$$

for which x is the *fast* variable and y is the *slow* variable. In the limit $\epsilon=0$ the xy system above becomes $0=xf(x,y,0), dy/dt=\zeta yg(x,y,0)$, referred to as the *$\epsilon$-slow subsystem*. It is a one-dimensional system restricted on the x nullcline, $0=xf(x,y,0)$. Under the change of time variable $t/\epsilon\to\tau$, referred to as the *ϵ-fast time*, the system becomes $dx/d\tau=xf(x,y,0), dy/d\tau=\epsilon\zeta yg(x,y,0)$. In the limit $\epsilon=0$, the system becomes $dx/d\tau=xf(x,y,0), dy/d\tau=0$, referred to as the *$\epsilon$-fast subsystem*. It is a one-dimensional system with y frozen as a parameter. The equilibrium point of this system is defined by $0=xf(x,y,0)$, i.e., the x nullcline.

Solutions of the fast subsystem are referred to as *fast solutions* or *fast orbits*. They are horizontal lines moving either to or away from the x-equilibrium points defined by the x nullcline. Similarly, solutions of the slow subsystem are referred to as *slow solutions* or *slow orbits*; however, they are oriented curves on the x nullcline. The solution curves either

Downloaded 10 Sep 2007 to 129.93.181.195. Redistribution subject to AIP license or copyright, see http://chaos.aip.org/chaos/copyright.jsp

move to or away from equilibrium points defined jointly by both the x and y nullclines, or move on a limit singular cycle as shown in Fig. 2. A detailed description follows below.

The x nullcline consists of two branches: the trivial branch $x=0$ and the nontrivial branch $0=f(x,y,0)$ (which can be explicitly solved for y as a function of x). Point $(1,0)$ in the nontrivial branch corresponds to the x-carrying capacity in the absence of predator y. With the increase of y as a parameter in the fast subsystem, the capacity in x continues but decreases. Thus the branch between the maximal point and the predator-free capacity $(1,0)$ is the predator-mediated carrying capacity, which satisfies analytically $f(x,y,0)=0, f_x(x,y,0)<0$. We call it the *descending capacity* branch of the nontrivial x nullcline, and denote it by p_{xdc}. It consists of stable equilibrium points of the x equation. The maximum point is called the *x-crash-fold* point, denoted by p_{xcf}, because for y immediately above it the fast x solution always collapses down to the extinction branch $x=0$. Mathematically, the x equation undergoes a saddle-node bifurcation at the crash-fold point as y changes. It is solved as $p_{\mathrm{xcf}}=((1-\beta_1)/2,(1+\beta_1)^2/4)$.

The remaining branch of the nontrivial x nullcline, left of p_{xcf}, is unstable for the fast x equation $(f=0, f_x>0)$. It represents the predator mediated capacity/extinction threshold in x. That is, for a fixed y, the prey grows to its predator-adjusted capacity p_{xdc} if it starts above the threshold and goes off to extinction if it starts below it. As the predation pressure increases from y the threshold in x increases. Thus we call it the *ascending threshold* and denote it by p_{xat}. Since the capacity branch p_{xdc} decreases as y increases, both must coalesce at a point in between, which is the crash-fold point p_{xcf}.

The intersection of the ascending threshold p_{xat} and the trivial x-nullcline branch $x=0$ is the emerging point of the capacity/extinction threshold. It is a *transcritical* bifurcation point where two distinct nullcline branches crisscross for the fast x subsystem as y changes. It is denoted by p_{xtc}, which is solved as $p_{\mathrm{xtc}}=(0,\beta_1)$. In general the nontrivial x nullcline, $0=f(x,y,0)$, is a parabola-like curve consisting of descending capacity, ascending threshold, and crash fold as branches and points.

Typical slow orbits always move down on the depleted resource branch $x=0$, but down or up on the capacity and threshold branch $f(x,y,0)=0$, depending on whether the resource amount x is smaller or larger than the amount to equilibriumize the y-slow equation. Solve the nontrivial y nullcline $g(x,y,0)=0$ to obtain $x=\beta_1\delta_1/(1-\delta_1)$, which represents the minimum amount of x required by the predator to grow. For this reason we call it the *growing threshold* and denote it by $x_{\mathrm{ygt}}=\beta_1\delta_1/(1-\delta_1)$. That is, for x immediately $>x_{\mathrm{ygt}}$, predator y increases $(dy/dt>0)$, and for x immediately $<x_{\mathrm{ygt}}$, it decreases $(dy/dt<0)$. The nontrivial y nullcline should usually be a curve on which x increases as y increases, representing an ascending y capacity, i.e., a greater (and fixed) amount of x sustains a greater amount of y at equilibrium. For our model, however, it becomes a degenerate vertical line $x=x_{\mathrm{ygt}}$, and this is the main reason for its name. As shown in Fig. 2(a), when y's growing threshold is greater than the amount to crash the prey but otherwise less than the carrying capacity, $x_{\mathrm{xcf}}<x_{\mathrm{ygt}}<1$, then all slow solutions on x's descending capacity branch converge to the xy-equilibrium point, which is the intersection of p_{ygt} and p_{xdc}.

The concatenation of fast and slow orbits are referred to as *singular orbits*. For the case shown in Fig. 2(a), it is a well-known fact that all singular orbits except for those from the axes will converge to the equilibrium point $p_{\mathrm{ygt}}\cap p_{\mathrm{xdc}}$. (Naturally, the attracting equilibrium point is referred to as an *equilibrium singular attractor*.) Understanding this phenomenon is useful for understanding the singular chaotic attractor under consideration. Before we do this, we first collect some terminology that will be used throughout the paper.

From the expression $x_{\mathrm{xcf}}=(1-\beta_1)/2$ we see that the formation of the x-crash-fold p_{xcf} takes place if, and only if, $\beta_1<1$. Since $\beta_1=a_1/K$, $\beta_1<1$ means that the predator is able to reach half of its maximum predation rate at a prey density a_1 smaller than the prey's carrying capacity. For this reason predator y is said to be *predatory efficient* if indeed it holds that $\beta_1<1$. Whether predator y is predatory efficient or not, is not essential for this paper. But it is the case for the z predator, which will be discussed later. Predator y is said to have a *low predatory-mortality rate* if it is predatory efficient and can actually crash the prey. That is, at the crash-fold state p_{xcf} the predator can grow in per capita: $g(x_{\mathrm{xcf}},y_{\mathrm{xcf}},0)>0$, which is solved as

$$x_{\mathrm{xcf}}=(1-\beta_1)/2>\beta_1\delta_1/(1-\delta_1)=x_{\mathrm{ygt}}.$$

It is easy to see that the predator's dimensionless mortality rate δ_1 should be relatively small as part of the requirement. Predator y is said to have a high predatory-mortality rate if otherwise $g(x_{\mathrm{xcf}},y_{\mathrm{xcf}},0)<0$.

The main reason that all singular orbits (except for those on the axes) will converge to the xy-equilibrium point when y is high in predatory-mortality rate [Fig. 2(a)] is counterintuitive in the case where singular orbits have a part on the axes. This in fact gave rise to a classic phenomenon in singular perturbations referred to as *Pontryagin's delay of loss of stability* (PDLS).[21–25]

2. Bust and boom dynamics

Take the case of singular orbits, which have a part on the y axis. More specifically, above the transcritical point $(0,y_{\mathrm{xtc}})$, the trivial equilibrium point $x=0$ of the x-fast equation is stable and below it; it is unstable. The PDLS phenomenon deals with the manner by which fast singular orbits jump away from the unstable trivial branch of the prey nullclines. In practical terms, the predator declines in a dire situation of depleted prey $x\approx 0$, followed by a surge in the prey's recovery after the predator reaches a sufficiently low density to allow it to happen. The mathematical question is how the critical predation density is determined. More specifically, let $(x_\epsilon,y_\epsilon)(t)$ be a solution to the perturbed equation with $\epsilon>0$ and an initial (a,b) satisfying $0<a<x_{\mathrm{xcf}}$ and b above the ascending threshold p_{xat} [Fig. 2(a)]. In the singular limit $\epsilon=0$, the orbit converges to a concatenation of two fast orbits and one slow orbit. The first fast orbit on $y=b$ collapses onto $x=0$; the second on $y=c$ for some c explodes toward p_{xdc}. According to the theory (see Refs. 19, 23, and

Downloaded 10 Sep 2007 to 129.93.181.195. Redistribution subject to AIP license or copyright, see http://chaos.aip.org/chaos/copyright.jsp

26 for a derivation), the critical amount c that allows x to recover is determined by the following integral equation:

$$\int_c^b \frac{f(0,s,0)}{sg(0,s,0)} ds = 0.$$

By substituting $s=y(t), y(0)=b$, the slow orbit on the trivial branch $x=0$, and observing that $ds/(sg(0,s,0))=dt$, the equation changes to $\int_{T_c}^{0} f(0,y(t),0)dt=0$, where T_c is the corresponding duration of flight $y(T_c)=c$. Because f is the per capita growth rate of the prey, which has opposite signs around the transcritical point y_{xtc}, and because the integral of f represents the accumulative per capita growth during the transition, this equation simply means that the critical point c is such that the prey's accumulative per capita growth rate over the growing phase $y<y_{\mathrm{xtc}}$ cancels it out over the declining phase $y>y_{\mathrm{xtc}}$. This is the so-called PDLS phenomenon and the critical amount c is denoted by $y_{\mathrm{xpd}}=c$. The PDLS quantity y_{xpd} depends on the initial b, which will be taken as the x-crash-fold level $b=y_{\mathrm{xcf}}$ most of the time, from now on. The case illustrated is for the type of transcritical points at which the fast variable goes through a phase of crash-recovery outbreak. (All PDLS points of our xyz model are of the crash-recovery-outbreak type.) We can now see from the phase portrait [Fig. 2(a)] that all singular orbits not from the axes will converge to the coexisting xy-equilibrium point.

The case of low predatory mortality ($x_{\mathrm{ygt}}<x_{\mathrm{xcf}}$) is illustrated in Fig. 2(b). In this case, all singular orbits not from the x axis will converge to the singular attractor of the limit cycle $ABCD$, for which B is the crash-fold point and D is the PDLS point. Its existence owes to the property that the predator can still grow at the crash-fold point ($x_{\mathrm{ygt}}<x_{\mathrm{xcf}}$). We point out that both the equilibrium and limit cycle singular attractors will persist for small $0<\epsilon\ll 1$ because of their hyperbolicity (see Refs. 13 and 16 for references on this question as well as the geometric method of singular perturbations in general). We will denote throughout this paper the landing point A of the x-fast orbit from D by $p_{\mathrm{xpd}}=A$ and refer to it as the PDLS point or the PDLS *capacity* point, and D the PDLS *outbreak* point instead to make the distinction.

3. Singular dynamics with stoichiometric limitation

We now consider the stoichiometrically mediated xz system with $y=0$: $\epsilon dx/dt=xf(x,0,z), dz/dt=z(E(x,0,z)x/(\beta_2+x)-\delta_2)$, where

$$E(x,y,z)=\min\left\{1,\frac{1-\sigma_1 y-\sigma_2 z}{\kappa x}\right\}.$$

The x-fast subsystem has the same structure as the xy subsystem when y is substituted by z. However, unlike the xy subsystem the first condition we impose on the xz subsystem assumes the following.

Condition 2. *z is predatory efficient* $0<\beta_2<1$.

Under this condition, there is a transcritical point p_{xtc}, a crash-fold point p_{xcf}, and a PDLS point p_{xpd}, respectively. The main difference lies in the z-slow subsystem, in particular the z nullcline.

The trivial branch $z=0$ is always there as with any other subsystem. The nontrivial branch $g(x,0,z)=E(x,0,z)x/(\beta_2+x)-\delta_2$ can be very different due to the stoichiometric factor $E(x,y,z)$, which is a variable reproductive efficiency factor. It divides the phase space into two parts: the *subsaturation* P:C region $E(x,y,z)<1$ and the *saturation* P:C region $E(x,y,z)=1$. The defining relations are equivalent to $1-\sigma_1 y-\sigma_2 z/\kappa x<1$ and $1-\sigma_1 y-\sigma_2 z/\kappa x\geq 1$, respectively. Recall that the quantity $1-\sigma_1 y-\sigma_2 z/\kappa x$ corresponds to the dimensionless P:C ratio for the growth of predator z. More importantly, being <1 of the ratio means that the predator's growth rate is below optimal for not having enough phosphorus or too much carbon. The line $1-\sigma_1 y-\sigma_2 z/\kappa x=1$ is the boundary of these two regions and we call it the *efficiency boundary* and denote it by p_{zeb}; see the dashed line in Fig. 2(c) through the point $(x_{\mathrm{zeb}},0,0)$ with $x_{\mathrm{zeb}}|_{\{y=z=0\}}=1/\kappa$. It is easy to see the ecological interpretation: below the efficiency boundary, x (in carbon) is relatively small and there is more than enough phosphorus to give z a saturated efficiency growth. The efficiency boundary decreases in x as z increases because more consumer z means less nutrient in phosphorus per consumer and thus it takes less resource in carbon to flip the consumer from a saturated efficiency growth to a subsaturated efficiency growth.

In the saturated efficiency region $E=1$, the nontrivial z nullcline is $x=x_{\mathrm{zgt}}=\beta_2\delta_2/(1-\delta_2)$ provided $x_{\mathrm{zgt}}<x_{\mathrm{zeb}}=1/\kappa$, which are solved from the equation $g(x,0,z)=x/(\beta_2+x)-\delta_2=0$ with $E=1$. Similar to the predator y without stoichiometric limitation, it represents the growing threshold for z: $dz/dt>0$ for x immediately greater than x_{zgt} and $dz/dt<0$ for x immediately smaller.

In the subsaturation efficiency region $E<1$, the nontrivial z nullcline is another line $(1-\sigma_2 z)/[\kappa(\beta_2+x)]-\delta_2=0$. It is an x-supported capacity equilibrium for the z equation: below it $dz/dt>0$ and above it $dz/dt<0$. It decreases in z as x increases because it is in the subsaturated efficiency region for which more carbon in the resource is less desirable, meaning low P:C ratio for the consumer. For a similar reason as for p_{xdc} we call it the *descending capacity* of the z predator and denote it by p_{zdc}. The x intercept is $x_{\mathrm{zdc}}|_{\{y=z=0\}}=1/(\kappa\delta_2)-\beta_2$, which is automatically $>x_{\mathrm{zeb}}|_{\{y=z=0\}}=1/\kappa$ because of the same condition $x_{\mathrm{zgt}}=\beta_2\delta_2/(1-\delta_2)<x_{\mathrm{zeb}}|_{\{y=z=0\}}=1/\kappa$.

The significance of this branch of the z nullcline lies in the fact that as x increases across the branch, z experiences a subsaturation efficiency growth ($dz/dt>0, E<1$) to a complete halt on the branch to a subsaturation efficiency decline ($dz/dt<0, E<1$) all because the resource carbon x becomes critically excessive. Because p_{zgt} is a vertical line and p_{zdc} decreases in x as z increases, they must intersect, and the intersection is the maximum point of the z nullcline, denoted by p_{zcf}, called the *capacity fold* point. In fact, both intersect on the efficiency boundary p_{zeb} and a simple calculation yields $p_{\mathrm{zcf}}|_{\{y=0\}}=(x_{\mathrm{zgt}},0,(1-\kappa x_{\mathrm{zgt}})/\sigma_2)$. The region to the left of the growing threshold p_{zgt} is referred to as the P*(phosphorus)-excessive region* (or the C*(carbon)-poor region*. The region between p_{zgt} and p_{zdc} is referred to as the P:C-*balanced region*. The region to the right of the descend-

Downloaded 10 Sep 2007 to 129.93.181.195. Redistribution subject to AIP license or copyright, see http://chaos.aip.org/chaos/copyright.jsp

ing capacity p_{zdc} is referred to as the P-*poor region* (or C-*excessive region*). The P:C-balanced region is the only region where z can grow ($dz/dt>0$).

The nontrivial z nullcline may or may not intersect the nontrivial x nullcline. More specifically, the growing threshold may not intersect the x nullcline more than once since it is a vertical line segment and for the latter z is a function of x. We will assume for this paper the following.

Condition 3. *The unique existence of an xz-equilibrium point p_{xzdt} on predator's growing threshold and prey's ascending threshold:* $x_{zgt}<x_{zeb}$, $x_{zgt}<x_{xcf}$, $f(x_{zgt},0,z_{zcf})<0$.

Here the first inequality guarantees that the existence of predator's growing threshold is in the saturated efficiency region. The second inequality is needed for the point to lie on x's ascending threshold. The third inequality indeed guarantees such an existence because z's capacity-fold point p_{zcf} lies above the x nullcline.

Because the nontrivial x -nullcline ($p_{xat}\cup p_{xdc}$) is a parabola and z's descending capacity curve p_{zdc} is a negative-sloped line, they can intersect at most at two points over the interval $0<x\leq 1$. If there is no intersection, then the singular orbit structure for the xz system is qualitatively the same as the xy system without the stoichiometric effect. The original system with the parameter values discussed in Sec. II belongs to the case of having two intersections of p_{xdc} and p_{zdc}. However, the mechanism for chaos generation is almost identical to the case of having just one intersection, which is the case we will consider from now on because of its relative simplicity. The precise condition for this case is as follows:

Condition 4. *The unique existence of an xz-equilibrium point on predator's and prey's descending capacities:* $x_{zdc}|_{\{y=z=0\}}=1/(\kappa\delta_2)-\beta_2<1$, $g(x_{xcf},0,z_{xcf})>0$.

The first inequality guarantees that there is only one xz-equilibrium point on z's capacity p_{zdc} and the second inequality makes sure the point is also on x's capacity p_{xdc} when z is low in predatory-mortality rate. We note that whether there is one or two xz-equilibrium points on predator's descending capacity p_{zdc}, the important point is that part of the x-carrying capacity p_{xdc} must lie in predator's P-poor region in which $dz/dt<0$. It is this unique stoichiometric property that ultimately determines the existence of the singular chaos attractor under consideration as we will demonstrate later.

The case satisfying all the conditions (1–4) so far is illustrated in Fig. 2(c). Both xz equilibrium points are unstable for the z subsystem. The singular attractor has two generic kinds. The equilibrium point $p_{xzdc}=p_{xdc}\cap p_{zdc}$ is always repelling. If it lies above the PDLS point, p_{xpd}, all singular orbits converge to the predator-free x-capacity equilibrium point $(1,0)$. In this case, the P-poor x-capacity region is substantial to be dynamically distinctive from the stoichiometry-free xy subsystem. If it lies below p_{xpd}, all singular orbits above the line $z=z_{xzdc}$ converge to a singular limit cycle through the x-crash-fold point, and all singular orbits below the line $z=z_{xzdc}$ converge to the predator-free x equilibrium. The latter case qualitatively resembles the xy dynamics as if there is no stoichiometric limitation on z as long as solutions do not start below the line $z=z_{xzdc}$. In other words, the P-poor x-capacity region is too small to make a substantial difference. It is the former case that we will consider in this paper as formalized below.

Condition 5. *The P-poor x-capacity region is relatively substantial to capture the PDLS capacity point:* $z_{xpd}<z_{xzdc}$.

We end this section by commenting on whether or not these conditions can satisfy simultaneously. Note first, that the singular parameters ϵ,ζ have nothing to do with the nullcline structures. So condition 1 does not affect the question one way or another. Second, the remaining conditions so far concern the xz subsystem and parameters $\beta_2,\delta_2,\sigma_2,\kappa$ only. The number of defining equations is 4: $\beta_2<1$, $x_{zgt}<x_{zeb}$, $x_{zdc}|_{\{y=z=0\}}<1$, $g(x_{xcf},0,z_{xcf})>0$ [with the last implying $f(x_{zgt},0,z_{zcf})<0$]. The number of parameters is also 4. Generically, the equations define a nonempty parameter region. For example, making δ_2 small will make the second inequality hold. Making κ large will make the third inequality to hold. Finally, decreasing σ_2 (and δ_2 if needed) will make the z-capacity-fold pointp_{zcf} to slide up on the vertical line $x=x_{zgt}$, hence making the last inequality to hold.

D. Multi-time-scale analysis: 3D case

We are now ready to consider the full system. Figure 3 highlights the essential configurations of the nullclines that give rise to the singular chaos attractor. We will build up the 3D configurations by piecing together properties from the lower-dimensional subsystems as building blocks. For example, on the $y=0$ section, the illustration simply reproduces that of Fig. 2(c) for the xz subsystem. Similarly, on the $z=0$ section, it reproduces that of Figs. 2(a) or 2(b). To fill in the remaining space between these coordinate planes, we will use the xz subsystems parametrized by variable y to sweep the effective first octant.

We first describe the full nontrivial x nullcline, which now is a cylindrical parabola-like surface, $f(x,y,z)=0$. At $y=0$ we already have its full description as a parabola going through $(1,0,0)$ with the crash-fold point p_{xcf}, the transcritical point p_{xtc}, and the PDLS point p_{xpd} due to condition 2. All these points will continue as parametrized by y. For example, increasing the density of y a little reduces the resource x originally allocated to z, and consequently it only takes a smaller amount of z to crash x. Therefore the continued x-crash-fold curve p_{xcf} decreases in z as y increases. This is easily seen when it is projected down to the yz plane as in Fig. 3(b). [This conclusion also follows by analyzing the defining equations $f(x,y,z)=0, f_x(x,y,z)=0$ as in Ref. 16.] The same yz-reciprocal relation also holds for the x-transcritical line p_{xtc}, which is explicitly expressed as $1-y/\beta_1-z/\beta_2=0$. The regions bounded by these curves and the coordinate planes, respectively, are the x-capacity surface p_{xdc}:$f(x,y,z)=0, f_x(x,y,z)<0$, which decreases in x as y or z increases; the x-threshold surface p_{xat}:$f(x,y,z)=0, f_x(x,y,z)>0$, which increases in x as y or z increases.

Last, the PDLS outbreak points are defined by two integral equations, one for each of the predator variables. Again, the projected points on x's descending capacity surface p_{xdc} are denoted by p_{xpd}, referred to as the PDLS points as before. For the type of nullcline configurations we need, we want the

Downloaded 10 Sep 2007 to 129.93.181.195. Redistribution subject to AIP license or copyright, see http://chaos.aip.org/chaos/copyright.jsp

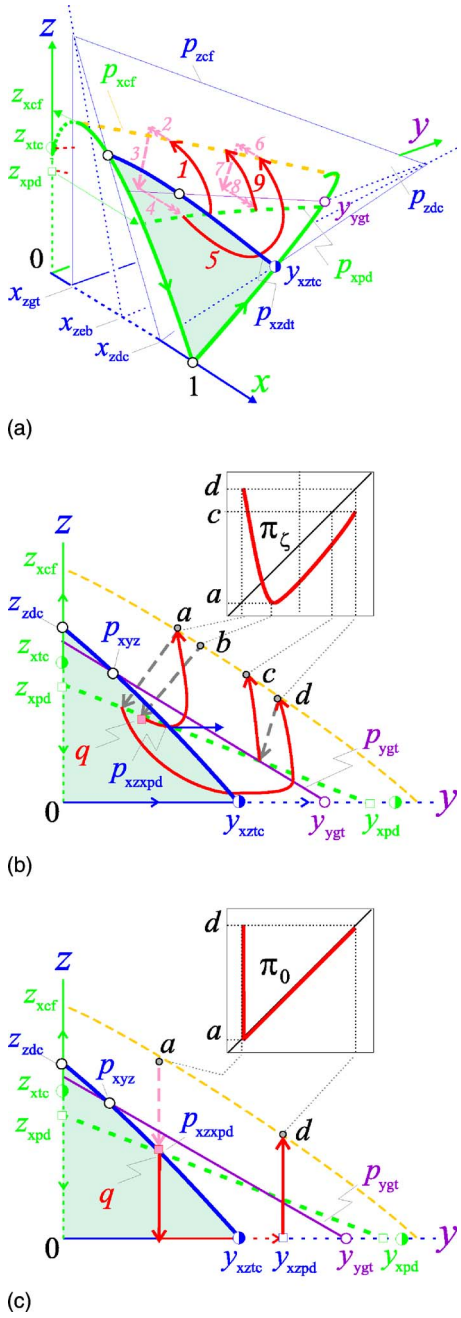

FIG. 3. (Color online) (a) A 3D view of the nullclines satisfying all the conditions 1–8, and a typical singular orbit. (b) The projected view onto the yz plane and the corresponding ϵ-singular return map π_ζ with $0<\zeta\ll 1$. (c) The ζ-limiting view of the perturbed case (b). Marker designation: Open circles are xyz equilibrium points; half-filled circles are transcritical points; open squares are PDLS points; filled-squares are junction-fold points.

PDLS curve to decrease in z when y increases, and vice versa. This reciprocal relation holds at the parameter values $\beta_1=\beta_2=1$, which can be directly verified that the corresponding transcritical line $(f(0,y,z)=1-y-z=0)$ and the crash fold $(f(x,y,z)=0, f_x(x,y,z)=0)$ coincide. Hence, the PDLS curve coincides with the transcritical line and the crash fold as well, for which the wanted reciprocal relation holds. Since the equations are infinitely smooth in the saturated efficiency region $E=1$, where the PDLS jump is defined, the same reciprocal relation holds for β_i near 1. We formalize this by the following condition.

Condition 6. *The PDLS curve on the x-capacity surface decreases in z as y increases.*

We consider next the y nullcline, which is a plane, $x=x_{ygt}$, parallel to the yz plane. Because singular orbits will eventually visit either the x-trivial branch $x=0$ or the capacity surface p_{xdc}, it is important to consider its intersection with the nontrivial x nullcline. Its intersection with x's ascending threshold p_{xat} has little consequence to this paper; its intersection with the descending capacity p_{xdc} does. The intersection is a curve continued from the xy-equilibrium point for the xy subsystem. Its projection to the yz plane is a line, since it is defined by $f(x_{ygt},y,z)=0$ for which y and z are reciprocally and linearly related. It represents a descending capacity or threshold for y according to our terminology convention: For fixed z it attracts the y solutions if it is on x's descending capacity p_{xdc}, and it repels the y solutions if it is on x's ascending threshold p_{xat}. In either case, it decreases in y as z increases due to z's competitive pressure [see Figs. 3(b) and 3(c)]. [Part of the curve should be denoted by p_{xydc} with the subscript standing for "the y-equation's descending capacity (equilibrium) on x's carrying capacity p_{xdc}" and the other part by p_{xydt}, interpreted accordingly.] However, this finer distinction will not be used further and for this reason we will use p_{ygt} and p_{xydc} interchangeably, should it cause little confusion.) We will come back for more discussion on where to position this curve to generate the singular chaos attractor we are after.

We now consider the z nullcline, which has two branches: the degenerate, unstable branch of the growing threshold p_{zgt}, and the stable, descending capacity branch p_{zdc}. The former lies in the saturated efficiency region $E=1$ and the latter in the subsaturation region $E<1$. Without competitor y, it intersects the x nullcline at two equilibrium points by conditions 2–4. These two points continue as a curve, each as y increases. By making δ_1 small enough we can make the intersection curve with z's growing threshold initially sufficiently away from x's crash-fold curve so that we do not need to deal with its inconsequential role later. The important feature of the z nullcline instead is the intersection of its descending capacity p_{zdc} with x's descending capacity p_{xdc}. Its projection to the yz plane is $h(\phi(y,z),y,z)=(1-\sigma_1 y-\sigma_2 z)/[\kappa(\beta_2+\phi(y,z))]-\delta_2=0$, with $E<1$ and $x=\phi(y,z)$ solved from $f(x,y,z)=0$. Using implicity differentiation, it is easy to show that for σ_i/κ modestly large y and z are reciprocal in relation on the curve by using the fact that $E<1, \phi_y<0, \phi_z<0$. It is actually easier to see this ecologically. The intersection represents an unstable threshold equilibrium for the slow z equation with y fixed on x's capacity surface p_{xdc}. This is the case when $y=0$ by condition 4 for which more of x means more excessive carbon for z, thus driving down z's density further from the equilibrium, giving rise to an unstable, threshold equilibrium. With a small increasing in y, the excessive amount of x is removed by y accordingly, becoming less excessive for z. Hence it takes a greater x amount to drive down z. That is, z's descending capacity is reduced on p_{xdc}. The condition that $\sigma_i\kappa$ is large simply guarantees that this z descending threshold continues down to $z=0$ as y increases. By our terminology convention, it is denoted by p_{xzdt}, standing for z's descending threshold

Downloaded 10 Sep 2007 to 129.93.181.195. Redistribution subject to AIP license or copyright, see http://chaos.aip.org/chaos/copyright.jsp

on x's capacity surface, even though the original branch for z is the descending capacity. We will use p_{xzdt} and p_{zdc} interchangeably since our analysis is entirely framed on x's capacity surface. The descending rate depends on y's dimensionless P:C ratio σ_1: the higher the ratio is the faster the descent becomes. This is an important property to be used below. In addition, the intersection of p_{xzdt} with the trivial z nullcline $z=0$ is a transcritical point p_{xztc} as shown in Fig. 3, for which the PDLS phenomenon takes place for the ζ singularly perturbed yz system on the resource capacity surface; see
Fig. 3(c) for its ramification.

One of the key configurations we are after is for z's x-supported descending threshold p_{xzdt} to intersect x's PDLS curve p_{xpd}. By condition 5, z's P-poor, x-capacity region (shaded in Fig. 3) captures the PDLS point when $y=0$, i.e., $z_{xpd}|_{\{y=0\}} < z_{xzdt}|_{\{y=0\}}$. For the intersection to take place we only need to show that the other end of the PDLS curve p_{xpd} at $z=0$ is outside the region or to the opposite side of its boundary p_{xzdt}, i.e.,

$$y_{xzdt}|_{\{z=0\}} < y_{xpd}|_{\{z=0\}}. \tag{7}$$

This indeed is the case because of the following. First we choose σ_1 large enough so that the transcritical point $p_{xztc}|_{\{z=0\}}$ lies below the x crash fold on the y axis, i.e., $y_{xzdt}|_{\{z=0\}} < y_{xcf}|_{\{z=0\}}$. To be precise, we can first pick σ_1, so that $y_{xztc}|_{\{z=0\}} < (1+s)^2/4$ with $s=0$ and with the right hand of the inequality from the expression of $y_{xcf}|_{\{z=0\}} = (1+\beta_1)^2/4$, which is independent of σ_1. After fixing this σ_1, we then increase β_1 (i.e., decrease the predatory efficiency of y), if necessary, so that the y end of x's transcritical point p_{xtc} is pushed towards x's crash-fold point. As a result, the y end of x's PDLS curve is pushed closer to x's crash-fold point. In fact, at $\beta_1=1$ the y end of the crash-fold point p_{xcf}, the transcritical point p_{xtc}, and the PDLS point p_{xdp}, all merge as one point for the xy subsystem because $x_{xcf}|_{\{z=0\}} = (1-\beta_1)/2$, and the relation $y_{xzdt}|_{\{z=0\}} < 1/4 < y_{xcf}|_{\{z=0\}} = y_{xtc}|_{\{z=0\}} = y_{xpd}|_{\{z=0\}} = 1$, holds. It will hold for a range of β_1 away from $\beta_1=1$ by continuity, and hence the relation (7) will hold. Note further that by increasing σ_1 further we can make sure the intersection is unique because we can make the descending rate of the threshold curve p_{xzdt} faster than the descending rate of the PDLS curve p_{xpd} (condition 6). This property is formalized as follows.

Condition 7. *The PDLS curve p_{xpd} intersects z's x-supported descending threshold p_{xzdt} at a unique point, denoted by $p_{xzxpd} = p_{xzdt} \cap p_{xpd}$, in the manner so that (7) holds (see Fig. 3).*

One important consequence of this configuration is that in z's P-poor region on x's capacity surface z decreases when started from that part of the PDLS curve, whereas in z's P:C-balanced region on p_{xdc}, z increases when started from this part of the PDLS curve. It is this dichotomy that essentially drives the ϵ-singular orbits to chaos as we demonstrate now.

Figure 3(a) illustrates this ϵ-singular chaos in a preliminary way. The initial point of the yz-slow orbit 1 is on the PDLS curve p_{xpd} and z's descending threshold p_{xzdt} on the x-capacity surface. Hence it develops parallel with the y axis initially, away from z's P-poor region and into its P:C-balance region, in which it moves up and hits the x-crash-fold line in a finite time. At that point the x-fast orbit 2 takes it to the resource depleted branch $x=0$, followed by the yz-slow orbit 3, which decreases in both y and z, to x's PDLS outbreak jump line. The x-fast orbit 4 then takes it to the PDLS curve on x's capacity surface again. Assume it lands left, where it started from orbit 1; that is, in z's P-poor region (a condition that guarantees this assumption will be given in the next section). Then the yz-slow orbit 5 will first decrease in z before horizontally crossing the P-poor region's boundary p_{xzdt} and then increases in z in the P:C-balanced region until hitting x's crash-fold again. This is to be followed by singular orbits 6, 7, 8, 9, and so on. Again, assume the fast x-PDLS orbit 8 lands left where it started from orbit 5 and the same for all subsequent singular cycles. Then, a train of such singular oscillations in the manner of Fig. 2(b) develops and moves leftward until hitting the P-poor region again, switching its direction southward like orbit 5 to start another round of such bursts of oscillation. The task that remains is to make this description precise.

E. Singular return maps

We will use Poincaré return maps to capture the dynamics of the singular attractor. Since the ϵ-singular dynamics is 2D, consisting of orbits of the reduced 2D, ϵ, slow yz equations on the x-capacity surface p_{xdc} and the trivial surface $x=0$, and orbits of the 1D, ϵ-fast x orbits, the return map is of 1D, which can be defined on any curve on the x-capacity surface p_{xdc} or the trivial surface $x=0$ that is transversal to the reduced yz-slow flows. For definiteness we will take the x-crash-fold curve as the domain of the return map, and denote the domain by I and the return map by π_ζ, which is ζ dependent. The domain I can be thought as an interval, parametrized by the y coordinate on the fold, and the return map as $y_{n+1} = \pi_\zeta(y_n)$ for $y_i \in I$. It is easier to describe the return map by looking into the x axis and view the 3D structure of Fig. 3(a) in its projection to the yz plane as in Figs. 3(b) and 3(c). The return map π_ζ is a unimodal map as depicted in Fig. 3(b) with one minimum point at $y=b$ as the unique critical point. To the left of b, π_ζ is decreasing and to the right it is increasing but below the diagonal line $y_{n+1} = y_n$. This property is due to the existence of a *junction fold* point,[13] which by definition is on the PDLS curve p_{xpd} and at which the reduced yz-vector field is tangent to the PDLS curve. A sufficient condition for the existence of such a point is the following.

Condition 8. *Let the x-supported y nullcline be $p_{xydc} = p_{ygt} \cap p_{xdc}$. Then it lies above the point p_{xzxpd}, defined from condition 7, i.e., $dy/dt > 0$ at p_{xzxpd}, and if p_{xydc} intersects either p_{xpd} or p_{xzdt} then it does so that $y_{xzdt}|_{\{z=0\}} < y_{xydc}|_{\{z=0\}} < y_{xpd}|_{\{z=0\}}$; see Fig. 3.*

A geometric paraphrasing of this condition goes as follows. That $dy/dt > 0$ at p_{xzxpd} holds automatically for $\delta_1 = 0$ because p_{xydc} coincides with p_{xtc} and because of condition 7. Increasing δ_1 pushes the curve p_{xydc} closer and closer to the PDLS point p_{xzxpd} on p_{xzdc} from above, maintaining the re-

Downloaded 10 Sep 2007 to 129.93.181.195. Redistribution subject to AIP license or copyright, see http://chaos.aip.org/chaos/copyright.jsp

lation $dy/dt>0$ at p_{xzxpd}. By making the x supported z nullcline p_{xzdt} steeper and p_{xpd} flatter if necessary we can make p_{xydc} approach the point p_{xzxpd} in the way required by condition 8 for all δ_1 from an interval $[0,\delta_1^*)$ for which $p_{xzxpd}\in p_{xydc}$ when $\delta_1=\delta_1^*$. In fact, as δ_1 tends to δ_1^* from below, p_{xydc} must intersect p_{xzdt} from some δ_1 value on and the intersection is a unique unstable xyz-equilibrium point $p_{xyz}=p_{xydc}\cap p_{xzdt}$. This point approaches p_{xzxpd} from above. As a result the return map π_ζ must goes through a cascade of period-doubling bifurcations to chaos. The precise statement is as follows.

Theorem 2. *If conditions 1–8 are satisfied, then for* $\epsilon=0$ *and each* $0<\zeta\ll 1$ *a cascade of period-doubling bifurcations must take place for the perturbed return map* π_ζ *as* δ_1 *changes over a subinterval of* $[0,\delta_1^*)$ *in which the x-capacity supported y nullcline* $p_{xydc}=p_{ygt}\cap p_{xdc}$ *lies above* p_{xzxpd}, *and* $|p_{xyz}-p_{xzxpd}|=O(1/|\ln\zeta|)$.

A proof can now be constructed by modifying the proof of Theorem 6.1 of Ref. 13 or the proof of Theorem 1.1 of Ref. 17. In fact, the geometric configuration established by conditions 1–8 as well as the manner by which the bifurcation takes place is qualitatively *identical* to both cited theorems. Here below we demonstrate why π_ζ is a unimodal map as we claimed in the last section.

Note that below the curve p_{xydc}, $dy/dt>0$ and above it, $dy/dt<0$. It is easy to show now the existence of a junction-fold point on the PDLS curve p_{xpd} by the intermediate value theorem. Specifically, at the $y=0$ end of the PDLS curve, the yz-vector field points to the down side of the PDLS curve. In contrast, at p_{xzxpd}, the p_{xzdt} end of the PDLS curve, the yz-vector field is horizontal, pointing to the opposite side of the PDLS curve because the point lies in the $dy/dt>0$ region by condition 8 above and the fact that p_{xpd} has a negative slope everywhere by condition 6. Hence there must be

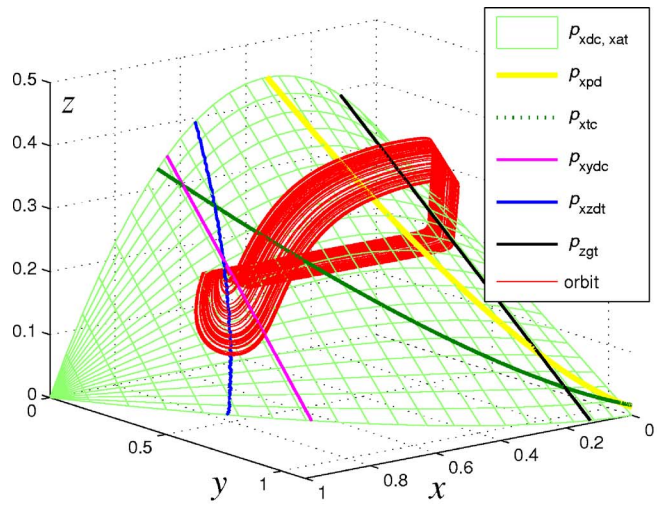

(a)

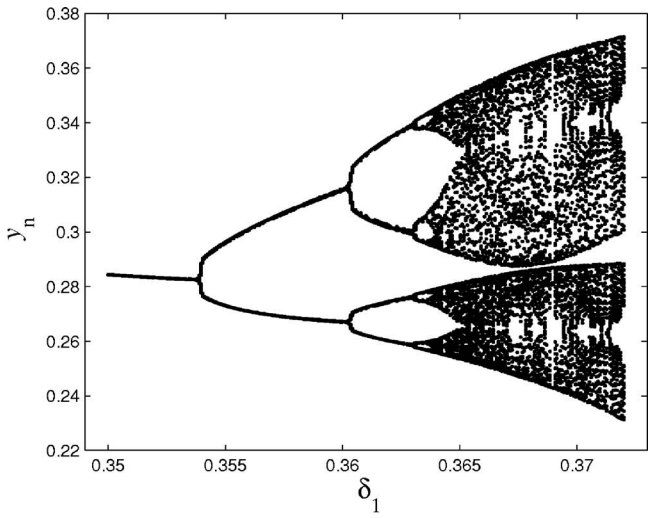

(c)

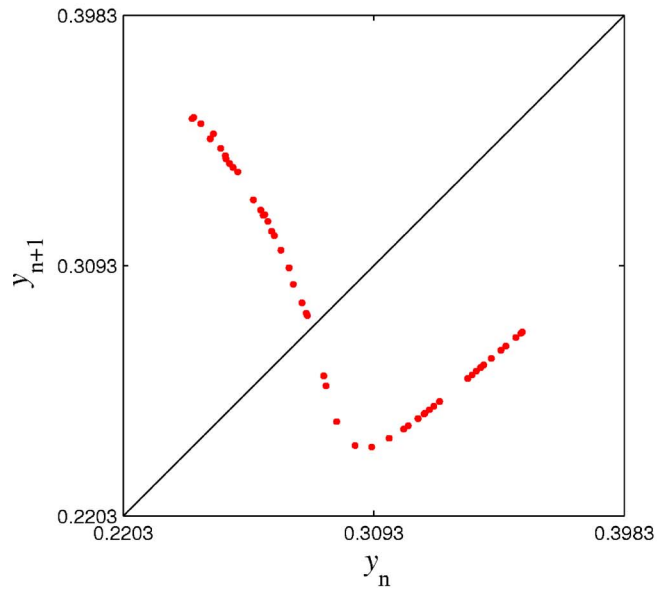

(b)

FIG. 4. (Color online) Parameter values for (a) and (b): $\epsilon=0.01$, $\zeta=0.12$, $\beta_1=1.1$, $\beta_2=0.33$, $\delta_1=0.368\,403$, $\delta_2=0.25$, $\sigma_1=0.2$, $\sigma_2=4/6$, $\kappa=20/6$. (a) A 3D phase portrait. (b) The Poincaré return map in coordinate y when z reaches a local maximum. (c) A bifurcation diagram for the same parameter value except for a range of δ_1 from $[0.35,0.372]$.

Downloaded 10 Sep 2007 to 129.93.181.195. Redistribution subject to AIP license or copyright, see http://chaos.aip.org/chaos/copyright.jsp

such a point q in between inside the P-poor region at which the yz-vector field is tangent with the PDLS curve, pointing to neither side of p_{xpd}.

The existence of the junction-fold point q implies the following. For points on the PDLS curve and left of q, the yz orbit moves below the curve first and then across it on the right of q. For PDLS points right of q, the yz orbit moves above the curve, never intersecting it again before hitting the x-crash-fold curve p_{xcf}. This effect leads to the unimodal property of the return map π_ζ at the minimum point b. To be more specific, point b is chosen so that its ϵ-singular orbit lands precisely on the junction-fold point q. Its returning image is a. Following any two points left of b, they all return to I with their relative position reversed because their yz-slow flows swing them half turn about the junction-fold point. Because the return map π_ζ reverses the orientation of the subinterval left of b, it is monotone decreasing in the subinterval. In contrast, for any pair of points right of b, their images by the return map π_ζ preserve their relative ordering because of the absence of a half twist by the yz flow around the junction-fold point q. Hence the map is monotone increasing on the right subinterval of b, implying that b is a global minimum for π_ζ.

The reason that the minimum point $(b,a)=(b,\pi_\zeta(b))$ lies below the diagonal for each $0<\zeta\ll 1$ so that $|p_{\mathrm{xyz}}-p_{\mathrm{xzxpd}}|\ll O(1/|\ln\zeta|)$ can be easily seen at the end point $\delta_1=\delta_1^*$ at which $p_{\mathrm{xyz}}=p_{\mathrm{xzxpd}}$ and the junction fold q coincides with p_{xzxpd} as well. As a consequence, all the yz orbits coming out right of the point q drift leftward without exception, so that the corresponding image of π_ζ is lower than its preimage, i.e., the graph of π_ζ over the right of $q=p_{\mathrm{xzxpd}}$ lies below the diagonal. All points left of $q=p_{\mathrm{xzxpd}}$ return to the right of the point.

On the other hand, when δ_1 is below and away from δ_1^*, the junction-fold q moves into the P-poor region and part of the subinterval right of q falls in the region where $dy/dt>0$, just like the left subinterval always does. The yz solution from q will first drift right, go vertical on p_{xydc}, and then drift left. Thus, if it accumulates more rightward drift than leftward drift, the minimum value of $a=\pi_\zeta(b)$ will lie above where it started, i.e., $b<a$. In this situation, a stable fixed point emerges in the right subinterval of b, giving rise to the starting cycle of the period-doubling cascade. This will happen for δ_1 sufficiently below δ_1^* so that $|p_{\mathrm{xyz}}-p_{\mathrm{xzxpd}}|=O(1/|\ln\zeta|)$.

Finally, the proof of the period-doubling cascade from the cited references was done by the theory of kneading sequences. In a nutshell, we calculate the symbol sequence (kneading sequence) of the minimum point b. Specifically, in one extreme when $\delta_1=\delta_1^*$, the symbol sequence is $LRR\ldots$, with L for the left interval and R for the right interval of b, and at least one R after L. In the other extreme when $|p_{\mathrm{xyz}}-p_{\mathrm{xzxpd}}|=O(1/|\ln\zeta|)$ for δ_1 sufficiently below δ_1^* for which π_ζ has an attracting fixed point in the right subinterval as explained above, the kneading sequence of b is $\bar{R}=RR\ldots$, a sequence of repeating Rs. From these two properties it is sufficiently to conclude by the theory of unimodal maps that in the intervening interval of δ_1 all the kneading sequences characteristic of the period-doubling cascade must take place and in the order prescribed by the cascade. Figure 4 gives an experimental validation to the scenario.

IV. DISCUSSION

We analyzed a chaos generating mechanism in a system, where two predators compete for one prey. A distinct feature of the system is its ability to track both prey quantity and prey quality (expressed as P:C content, i.e., stoichiometry, of prey). The variation in prey quality results in an unusual, hump-shaped consumer null surface. Yet, the particular intersection of all three species' null surfaces considered is qualitatively similar in configuration to a type found in a simple tritrophic food chain model for which at least four distinct types of chaos generation mechanisms have been classified.[13,18–20] This type is the simplest kind resulted from the existence of a junction-fold point on the consumer-mediated prey capacity. We find that both consumers can coexist on one prey in an attractor that, as we have shown both numerically and analytically, is chaotic. The chaos would not be possible without the stoichiometric mediation when prey quality negatively limits the growth of at least one consumer. However, other chaos generating mechanisms are possible in this stoichiometric competition model.

We note that the system exhibits stabilization mechanisms in which chaotic attractor collapses to a stable equilibrium. The manner by which this stabilization occurs is interesting—when a predator becomes more efficient with lowering death rate. We know that for a tritrophic food chain model, top consumers' reproductive efficiency plays an important role in similar stabilizations.[27] Likewise, we should expect the same stabilizing principle to prevail in the considered model. That is, increasing the relative efficiency rates ϵ and $\epsilon\zeta$ of the consumers against the prey should change the chaotic oscillations to small periodic oscillations and eventually to coexisting equilibrium states. Proving this stabilization principle as well as classifying all stoichiometrically generated chaos remains to be worked out.

[1] A. J. Lotka, *Elements of Physical Biology* (Williams and Wilkins, Baltimore, 1925) [reprint *Elements of Mathematical Biology* (Dover, New York, 1956)].
[2] J. Urabe and R. W. Sterner, "Regulation of herbivore growth by the balance of light and nutrients," Proc. Natl. Acad. Sci. U.S.A. **93**, 8465–8469 (1996).
[3] W. A. Nelson, E. McCauley, and F. J. Wrona, "Multiple dynamics in a single predator-prey system: experimental effects of food quality," Proc. R. Soc. London, Ser. B **268**, 1223–1230 (2001).
[4] J. Urabe, J. Togari, and J. J. Elser, "Stoichiometric impacts of increased carbon dioxide on planktonic herbivores," Glob. Change Biol. **9**, 818–825 (2003).
[5] T. Andersen, *Pelagic Nutrient Cycles: Herbivores as Sources and Sinks* (Springer-Verlag, Berlin, 1997).
[6] I. Loladze, Y. Kuang, and J. J. Elser, "Stoichiometry in producer-grazer systems: Linking energy flow with element cycling," Bull. Math. Biol. **62**, 1137–1162 (2000)
[7] E. B. Muller, R. M. Nisbet, S. A. L. M. Kooijman, J. J. Elser, and E. McCauley, "Stoichiometric food quality and herbivore dynamics," Ecol. Lett. **4**, 519–529 (2001).
[8] S. R. Hall, "Stoichiometrically explicit competition between grazers: species replacement, coexistence, and priority effects along resource supply gradients," Am. Nat. **164**, 157–172 (2004).
[9] I. Loladze, Y. Kuang, J. J. Elser, and W. F. Fagan, "Competition and

Downloaded 10 Sep 2007 to 129.93.181.195. Redistribution subject to AIP license or copyright, see http://chaos.aip.org/chaos/copyright.jsp

stoichiometry: coexistence of two predators on one prey," Theor Popul. Biol. **65**, 1–15 (2004).
[10]R. A. Armstrong and R. McGehee, "Competitive exclusion," Am. Nat. **115**, 151–170 (1980).
[11]W. Liu, D. Xiao, and Y. Yi, "Relaxation oscillations in a class of predator-prey systems," J. Differ. Equations **188**, 306–331 (2003).
[12]J. Huisman and F. J. Weissing, "Biodiversity of plankton by species oscillations and chaos," Nature **402**, 407–410 (1999).
[13]B. Deng, "Food chain chaos due to junction-fold point," Chaos **11**, 514–525 (2001).
[14]W. A. Calder III, "An allometric approach to population cycles of mammals," J. Theor. Biol. **100**, 275–282 (1983).
[15]W. A. Calder III, "Ecological scaling: mammals and birds," Annu. Rev. Ecol. Syst. **14**, 213–230 (1983).
[16]B. Bockelman, B. Deng, E. Green, G. Hines, L. Lippitt, and J. Sherman, "Chaotic coexistence in a top-predator mediated competitive exclusive web," J. Dyn. Differ. Equ. **16**, 1062–1092 (2004).
[17]B. Deng, "Glucose-induced period-doubling cascade in the electrical activity of pancreatic β-cells," J. Math. Biol. **38**, 21–78 (1999).
[18]B. Deng and G. Hines, "Food chain chaos due to Shilnikov's orbit," Chaos **12**, 533–538 (2002).
[19]B. Deng and G. Hines, "Food chain chaos due to transcritical point," Chaos **13**, 578–585 (2003).
[20]B. Deng, "Food chain chaos with canard explosion," Chaos **14**, 1083–1092 (2004).
[21]L. C. Pontryagin, "Asymptotic behavior of solutions of systems of differential equations with a small parameter at higher derivatives," Izv. Akad. Nauk SSSR, Ser. Mat. **21**, 605–626 (1957) (in Russian).
[22]M. A. Shishkova, "Investigation of a system of differential equations with a small parameter in the highest derivatives," Sov. Math. Dokl. **14**, 483–487 (1973).
[23]S. Schecter, "Persistent unstable equilibria and closed orbits of a singularly perturbed equation," J. Differ. Equations **60**, 131–141 (1985).
[24]A. I. Neishtadt, "Prolongation of the loss of stability in the case of dynamic bifurcations, I," Diff. Eq. **23**, 1385–1391 (1987).
[25]A. I. Neishtadt, "Prolongation of the loss of stability in the case of dynamic bifurcations, II," Diff. Eq. **24**, 171–176 (1988).
[26]A. K. Zvonkin and M. A. Shubin, "Non-standard analysis and singular perturbations of ordinary differential equations," Russ. Math. Surveys **39**, 69–131 (1984).
[27]B. Deng, "Equilibriumizing all food chain chaos through reproductive efficiency," Chaos 16, 043125 (2006).

Downloaded 10 Sep 2007 to 129.93.181.195. Redistribution subject to AIP license or copyright, see http://chaos.aip.org/chaos/copyright.jsp